JOC The Journal of Organic Chemistry

pubs.acs.org/joc Article

N-Vinyl and *N*-Aryl Hydroxypyridinium Ions: Charge-Activated Catalysts with Electron-Withdrawing Groups

George F. Riegel and Steven R. Kass*

Cite This: *J. Org. Chem.* 2020, 85, 6017−6026 Read Online

ACCESS | Metrics & More | Article Recommendations | Supporting Information

ABSTRACT: Charge-enhanced Brønsted acid organocatalysts with electron-withdrawing substituents were synthesized, and their relative acidities were characterized by computations, 1:1 binding equilibrium constants ($K_{1:1}$) with a UV−vis active sensor, ^{31}P NMR shifts upon coordination with triethylphosphine oxide, and in one case by infrared spectroscopy. Pseudo-first-order rate constants were determined for the Friedel−Crafts alkylations of *N*-methylindole with *trans*-*β*-nitrostyrene and 2,2,2-trifluoroacetophenone and the Diels−Alder reaction of cyclopentadiene with methyl vinyl ketone. These results along with kinetic isotope effect determinations revealed that the rate-determining step in the Friedel−Crafts transformations can shift from carbon−carbon bond formation to proton transfer to the catalyst's conjugate base. This leads to an inverted parabolic reaction rate profile and slower reactions with more acidic catalysts in some cases. Electron-withdrawing groups placed on the *N*-vinyl and *N*-aryl substituents of hydroxypyridinium ion salts lead to enhanced acidities, more acidic catalysts than trifluoroacetic acid, and a linear correlation between the logarithms of the Diels−Alder rate constants and measured $K_{1:1}$ values.

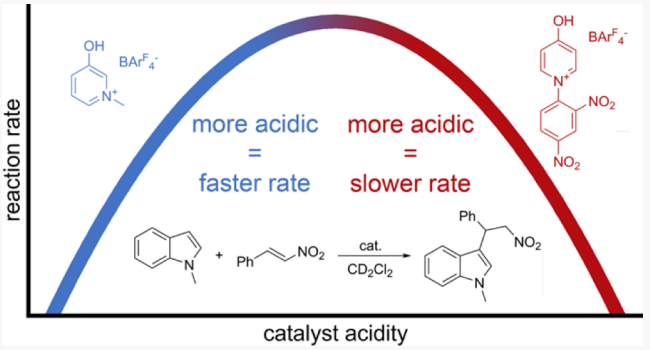

INTRODUCTION

Acid-catalyzed reactions are commonplace and are utilized in a wide variety of transformations spanning from the synthesis of small molecules to biocompounds and polymers. The development of Brønsted acids and hydrogen bond-donating organocatalysts, consequently, is of significant interest and a subject of considerable research efforts.[1,2] Incorporation of electron-withdrawing groups into these species not only increases their acidities and hydrogen bond donor abilities but also typically leads to more active catalysts and enhanced reaction rates.[3,4] Extension of this strategy with the use of one or more positively charged centers was recently reported to be particularly effective in nonpolar solvents, leading to rate accelerations corresponding to orders of magnitude compared to noncharged substituents.[5] Even more active catalysts can be envisioned by introducing electron-withdrawing groups into positively charged substrates. To explore this idea, a series of six model hydroxypyridinium salts were examined (**1**−**6**, Figure 1). In this report, we describe the syntheses of these [illegible] companion density functional theory computations, infrared (IR), UV−vis, and ^{31}P NMR spectroscopic studies, along with kinetic isotope effect (KIE) and rate constant determinations to assess catalyst acidities, activities, and reaction mechanisms.

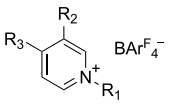

	R_1	R_2	R_3
1	Me	OH	H
2	(*E*)-CH=CHCO$_2$Et	OH	H
3	(*E*)-CH=CHCO$_2$Oct	OH	H
4	2,4-(NO$_2$)$_2$Ph	OH	H
5	(*E*)-CH=CHCN	OH	H
6	2,4-(NO$_2$)$_2$Ph	H	OH

Figure 1. Catalysts used in this work.

RESULTS AND DISCUSSION

The tetrakis[3,5-bis(trifluoromethyl)phenyl]borate ($BAr^F_4^-$) salt of the *N*-*n*-octyl-3-hydroxypyridinium ion has previously been reported,[5a] and its *N*-methyl analogue (**1**) was made in a similar way.[5d] Various strategies were employed for the preparation of the halide precursors of the other model species. Compound **2-Cl** was synthesized via a modification of the procedure from Jung and Buszek,[6] whereas **3-Cl** was formed using an analogous method to Katritzky et al.[7] The preparation of **5-Br** was accomplished using a similar

Received: February 25, 2020
Published: April 8, 2020

https://dx.doi.org/10.1021/acs.joc.0c00498
J. Org. Chem. 2020, 85, 6017−6026

procedure to that of Eicher-Lorka et al.,[8] and the 2,4-dinitrophenyl-substituted catalyst precursors, **4-Cl** and **6-Cl**, were obtained via a similar route to that reported by Eda, Kurth, and Nantz.[9] Conversions of the halide salts to their $BAr^F_4{}^-$ analogues were carried out largely in the same way and took advantage of the differential solubilities of NaCl and NaBr compared to $NaBAr^F_4$ in organic solvents.

Catalyst acidities were first evaluated at 298 K in the gas phase without the $BAr^F_4{}^-$ counteranion using B3LYP/6-31G(d,p) computations (Table 1). This methodology was

Table 1. Computed B3LYP/6-31G(d,p) Acidities for a Series of Catalysts without Their Counteranions[a]

catalyst	ΔG°_{acid}	$\Delta\Delta G^\circ_{acid}$
1	232.9	0.0
2	230.9	−2.0
4	226.6	−6.3
5	224.2	−8.7
6	219.3	−13.6

[a]All values are given in kcal mol^{-1} at 298 K. Smaller numbers for ΔG°_{acid} correspond to stronger acids.

previously used to reproduce experimental Brønsted acidities and successfully predict catalyst activities in nonpolar media.[5a] As anticipated, the presence of vinyl and aryl substituents with electron-withdrawing groups at the nitrogen ring center leads to more acidic species than their alkyl-substituted counterpart (i.e., **1**). In addition, **6**, the para-substituted analogue of **4**, is the strongest acid in this series because of enhanced electron delocalization in its conjugate base.

Several spectroscopic approaches were carried out to experimentally evaluate the relative acidities and hydrogen bond-donating abilities of **1**−**6**. IR spectroscopy was initially explored as previously reported by observing the change between the O−H stretching frequency of a phenol in carbon tetrachloride and upon coordination with 1% v/v CD_3CN in CCl_4.[5a,d] A reduction in this mode from 3541 to 3128 cm^{-1} was observed for **3**, and this difference of 413 cm^{-1} is larger than 370 cm^{-1} reported for *N*-*n*-octyl-3-hydroxypyridinium BAr^F_4.[5a] This result is consistent with an acidity enhancement because of the presence of an electron-withdrawing group, but **2** and **4**−**6** are not soluble in carbon tetrachloride or in CD_3CN/CCl_4 mixtures with up to 5% acetonitrile-d_3. Consequently, we decided to focus on alternative approaches.

A UV−vis titration method for evaluating hydrogen bond donor ability utilizing 7-methyl-2-phenylimidazo[1,2-*a*]-pyrazine-3(7*H*)-one (**7**) as a colorimetric sensor was first reported by Kozlowski and co-workers and recently updated by Payne and Kass.[5d,10] In the latter approach, a constant concentration of **7** is maintained as it is titrated with a Brønsted acid of interest (HOAr in this case). This leads to a blue shift of the λ_{max} of **7** because of its coordination with the hydrogen bond donor. When a 1:1 association occurs (Scheme 1), an isosbestic point is observed (Figures 2 and S8−S11), and a nonlinear fit of the data affords the equilibrium binding constant ($K_{1:1}$, Table 2). This was the case for **1**, **2**, **4**, and **5**. An isosbestic point is not observed for this last compound (Figure 3), which is indicative of the formation of two intermediate species, and is consistent with the resulting 1:2 binding model fit of the titration results. A plot of the logarithm of $K_{1:1}$ versus ΔG°_{acid} (Figure 4) is linear for all five hydroxypyridinium ion salts examined in this work,

Scheme 1. Coordination of 7 To Afford 1:1 and 1:2 Binding Complexes

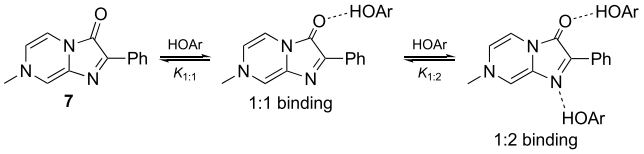

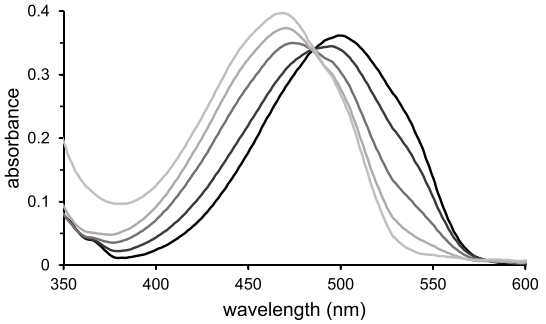

Figure 2. UV−vis spectra from 350 to 600 nm for the titration of **7** with **4**. Only some of the spectra are provided for clarity.

Table 2. Nonlinear Binding Isotherm Titration Results for a Series of Catalysts with 7[a]

catalyst	$\lambda_{max(1:1)}$ (nm)[b]	$K_{1:1}$	$K_{1:2}$
1[c]	472.1 (471.7)	2.0×10^4	
2	469.4 (468.8)	5.3×10^4	
4	469.1 (468.8)	8.5×10^4	
5	466.3 (466.0)	1.7×10^5	
6	434.7	3.5×10^5	7.2×10^3

[a]Constant sensor concentrations of 22−34 μM in CH_2Cl_2 were used. [b]Calculated values obtained from a plot of χ/λ_{max} at each titration point, where χ is the 1:1 mole fraction resulting from the fit of the data. See ref 5d for further details. Parenthetical numbers are the directly observed λ_{max} values from the titrations. [c]Data from ref 5d.

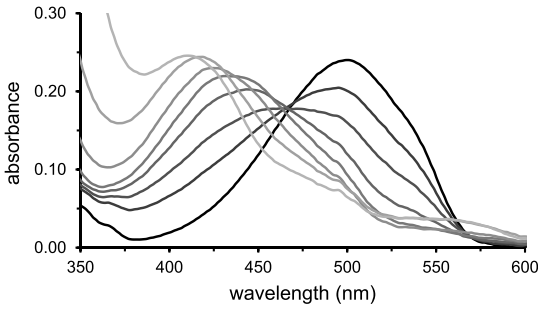

Figure 3. UV−vis spectra from 350 to 600 nm for the titration of **7** with **6**. Only some of the spectra are provided for clarity.

indicating that the 1:1 binding equilibrium constants provide a good measure of the catalyst acidities and hydrogen bond-donating abilities.[11]

An alternative spectroscopic approach for evaluating Brønsted acidities and hydrogen bond-donating abilities in nonpolar media was reported by Diemoz and Franz this past year.[12] In this methodology, the ^{31}P NMR spectrum of triethylphosphine oxide (Et_3PO) is recorded in dichloromethane and subsequently titrated with a Brønsted acid of interest. Rapid formation of a hydrogen bond complex leads to an averaged spectrum with a single downfield ^{31}P signal. Its

https://dx.doi.org/10.1021/acs.joc.0c00498
J. Org. Chem. 2020, 85, 6017−6026

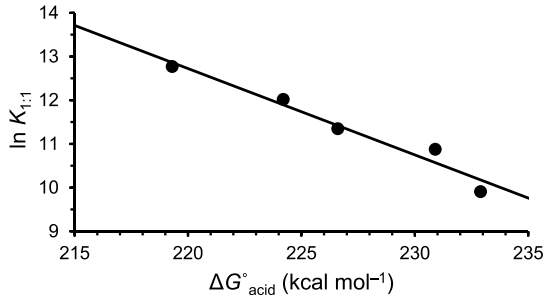

Figure 4. Logarithm of 1:1 equilibrium binding constants vs computed gas-phase acidities. A linear least-squares analysis affords $\ln K_{1:1} = -0.198 \times \Delta G^{\circ}_{acid} + 56.2$, $r^2 = 0.959$.

chemical shift progressively increases until it levels off to a constant value as more of the acid is added and the proportion of free (noncomplexed) Et_3PO diminishes to negligible amounts. The magnitude of this shift ($\Delta\delta$) was found to correlate with the activity of a variety of organocatalysts. For **1**, it was found that only 1.5 equiv are needed to bind to Et_3PO to achieve the maximum downfield shift (Table S7). Because all of our other catalysts are predicted to be more acidic than **1**, 1.5 equiv of these acids were considered to be sufficient to obtain the chemical shifts of the bound complexes (i.e., $\delta_{1.5}$). A summary of the results is given in Table 3, and $\Delta\delta$ for the

Table 3. Titration Results for a Series of Catalysts with Et_3PO Monitored by ^{31}P NMR[a]

catalyst	$\delta_{1.5}$ (ppm)[b]	$\Delta\delta$ (ppm)
1	60.83	10.33
2	61.67	11.17
4	61.96	11.46
5	62.49	11.99
6	65.44	14.94

[a]Triethylphosphine oxide (5.0 mM) in CD_2Cl_2 has a chemical shift of 50.50 ppm. [b]Observed chemical shifts upon addition of 1.5 equiv of the indicated acid.

meta-substituted isomers (**1**, **2**, **4**, and **5**) were found to linearly correlate with $\ln K_{1:1}$ from the UV–vis data (Figure 5) and ΔG°_{acid} (i.e., the computed gas-phase acidities, Figure S14). The para-substituted derivative shows positive deviations from the lines in both plots, presumably because of its enhanced acidity and hydrogen bond-donating ability because of the

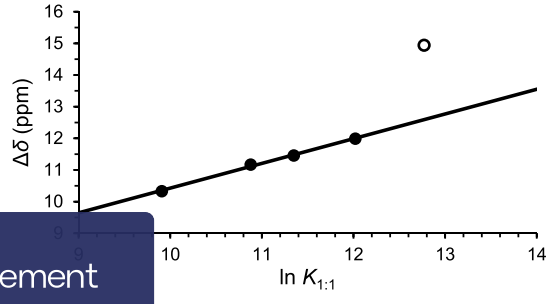

Figure 5. Triethylphosphine oxide ^{31}P NMR shift changes vs $\ln K_{1:1}$ for meta-substituted catalysts (filled circles) and **6** (open circle). A linear least-squares fit for the meta compounds gives the following equation: $\Delta\delta$ (ppm) = $0.781 \times \ln K_{1:1} + 2.62$, $r^2 = 0.997$.

conjugation of the acidic site with the formally charged nitrogen atom center.

Computations, 1:1 equilibrium binding constants from UV–vis titrations, and the triethylphosphine oxide ^{31}P NMR data all predict a catalyst activity order of **6** > **5** > **4** > **2** > **1**. To assess this prognostication, the Friedel–Crafts alkylation of *N*-methylindole with *trans*-β-nitrostyrene (eq 1) was examined.

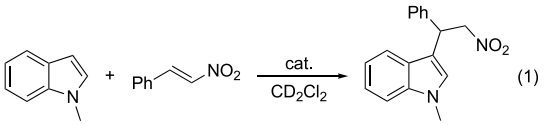

(1)

This reaction was chosen because it is known to progress more rapidly with stronger acids in a related series and has been widely used to assess organocatalysts.[5,12,13] Pseudo-first-order rate constants were obtained using ^1H NMR to monitor the reaction progress (Table 4). The reaction rates increased as

Table 4. Kinetic Data for the Friedel–Crafts Alkylation of *N*-Methylindole with *trans*-β-Nitrostyrene[a]

entry	catalyst	k (h^{-1})	$t_{1/2}$ (h)	k_{rel}
1		1.9×10^{-4}	3700	0.0023
2	**1**	0.082	8.5	1.0
3	**2**	0.17	4.2	2.0
4	**4**	0.19	3.6	2.4
5	**5**	0.29	2.4	3.6
6	**6**	0.21	3.3	2.6
7	TfOH	0.0088	79	0.11

[a]Reactions were carried out at 27 °C in CD_2Cl_2 with 10 mol % of the indicated catalyst, 500 mM *trans*-β-nitrostyrene, and 50 mM *N*-methylindole. Rate constants are corrected for the noncatalyzed background process.

expected for the meta-substituted pyridinium salts (i.e., **5** > **4** > **2** > **1**), but surprisingly, **6** afforded a smaller rate acceleration than **5** by a factor of 1.4, despite the former's greater acidity, larger $K_{1:1}$, and bigger $\Delta\delta$. Triflic acid was also examined, and it was found to be less active than our phenol derivatives and a poor catalyst for this transformation. This led us to hypothesize that for the stronger acids the carbon–carbon bond-forming step in the Friedel–Crafts alkylation may no longer be rate-determining and that deprotonation at C3 to aromatize the indole and reform the catalyst could become the slow step (Scheme 2). Such variations with changing pH are well-known and have been reported with organocatalysts[14] but not for the Friedel–Crafts reaction of *N*-methylindole with *trans*-β-nitrostyrene even though it has been extensively used for benchmarking purposes.

To probe a possible change in the rate-determining step of the mechanism, isotopically labeled 3-deuterio-*N*-methylindole[15] was prepared and KIEs for the Friedel–Crafts alkylation with different catalysts were determined (Table 5). An inverse KIE was obtained with **4**, and this is consistent with a rate-determining carbon–carbon bond-forming step (i.e., a change in hybridization from sp^2 to sp^3 in the nucleophilic attack of *N*-methylindole on *trans*-β-nitrostyrene). Conversely, normal KIEs were found with **6** and triflic acid. This is in accord with the deprotonation at C3 becoming the slow step in the reaction mechanism when more acidic catalysts are used. No isotope effect was found with **5**, suggesting that nucleophilic attack and deprotonation are competitive in this case. In

https://dx.doi.org/10.1021/acs.joc.0c00498
J. Org. Chem. 2020, 85, 6017–6026

Scheme 2. Proposed Reaction Mechanism for the Friedel–Crafts Alkylation of *N*-Methylindole with *trans*-β-Nitrostyrene Where Step 3 Becomes Rate-Determining with Strong Acid Catalysts.

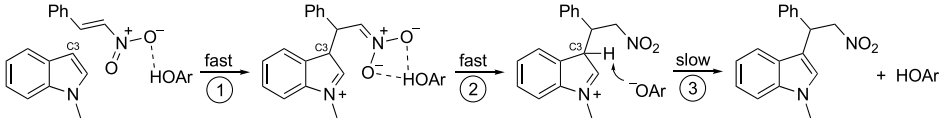

Table 5. Kinetic Data for the Friedel–Crafts Alkylation of 3-Deuterio-*N*-methylindole with *trans*-β-Nitrostyrene[a]

entry	catalyst	k_D (h^{-1})	$t_{1/2}$ (h)	KIE
1	**4**	0.24	2.8	0.80
2	**5**	0.29	2.4	1.0
3	**6**	0.13	5.2	1.6
4	TfOH	0.0050	138	1.7

[a]Background-corrected initial rates corresponding to reaction conversions of ≤10% were obtained at 27 °C in $CDCl_2$ using 50 mM 3-deuterio-*N*-methylindole, 500 mM *trans*-β-nitrostyrene, and 10 mol % of the indicated catalyst.

accord with the proposed mechanism in Scheme 2, ^2H NMR experiments showed that deuterium was only incorporated into the product at the α-position to the nitro group and was not observed until greater than 10% conversion to the product was reached. These findings reveal that the reaction rate for the Friedel–Crafts alkylation is not a reliable indicator of relative acidities for acidic catalysts.

It was anticipated that a more acidic intermediate in the Friedel–Crafts reaction is formed when 2,2,2-trifluoroacetophenone is used as the electrophile in lieu of *trans*-β-nitrostyrene. Two electron-withdrawing groups are present in the former case rather than one (i.e., OH and CF_3 vs NO_2), and they both are one bond closer to the key C3 position. This should facilitate the rearomatization step (3 in Scheme 2), making it more likely that carbon–carbon bond formation will be rate-determining and increasing the acidity range of catalysts that can be reliably probed. Mono- and bis-coupled products are commonly observed for this transformation (eq 2),[16] and so, the selectivities along with the reaction rate

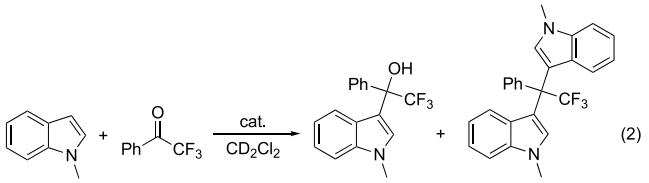

constants are given in Table 6 for the least (**1**) and most (**5**, **6**, and TfOH) acidic catalysts that were explored in this study. As expected, the KIEs are smaller for each catalyst, and this transformation proceeds 3.5 times more rapidly with **6** than with **5**. Formation of the bis-coupled product increases with the catalytic activity, suggesting that the mono/bis ratio can also serve as an indicator of the catalyst relative acidities. Tunable catalysts with modular syntheses such as our hydroxypyridinium salts are useful for this type of reaction because the proper balance between the reaction rate and selectivity must be struck.

To avoid multistep mechanisms where the rate-determining step can change with the acidity of the catalyst and to examine a model transformation that better reflects the Brønsted acidity and hydrogen bond-donating ability of the catalyst, the Diels–Alder reaction between cyclopentadiene and methyl vinyl ketone (MVK) was examined (eq 3). Pseudo-first-order rate

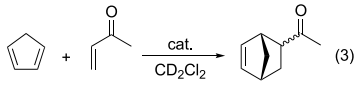

constants and the endo/exo product ratios were measured at 25 °C in dichloromethane-d_2 with a 1 mol % catalyst loading (Table 7). As expected based upon the computed acidities and

Table 7. Kinetic and Selectivity Data for the Diels–Alder Reaction of Cyclopentadiene with MVK[a]

entry	catalyst	k (h^{-1})	$t_{1/2}$ (h)	k_{rel}	endo/exo
1		0.11	6.5	0.72	86:14
2	**1**	0.15	4.7	1	89:11
3	**4**	0.46	1.5	3.1	91:9
4	**5**	0.81	0.85	5.5	91:9
5	**6**	3.4	0.20	23	92:8

[a]Reactions were carried out at 25 °C in CD_2Cl_2 with 1 mol % of the indicated catalyst, 250 mM cyclopentadiene, and 25 mM MVK. Background-corrected rate constants for the noncatalyzed process are given.

UV–vis and ^{31}P NMR data, the reactivity order is now **6** > **5** > **4** > **1** and the selectivities follow a similar trend. Excellent correlations between ln *k* and Δδ, ln $K_{1:1}$, and ΔG°_{acid} are observed (Figures 6, S15, and S16), indicating that all three approaches can serve as useful guides for catalytic activities.

A comparison of the charge-activated catalysts with noncharged species would be useful to obtain a better sense of their qualitative acidities. Pentafluorophenol (C_6F_5OH) and

Table 6. Kinetic and Selectivity Data for the Friedel–Crafts Reaction of *N*-Methylindole with 2,2,2-Trifluoroacetophenone[a]

entry	cat.	k_H (h^{-1})	$t_{1/2}$ (h)	k_{rel}	mono/bis[b]	k_D (h^{-1})[c]	$t_{1/2}$ (h)	k_H/k_D
1		7.4×10^{-5}	9400	0.0010	100:0			
2	1	0.072	10	1	100:0			
5		0.34	2.1	4.6	98:2	0.38	1.8	0.90
6		1.1	0.61	16	91:9	0.95	0.73	1.2
TfOH		0.053	13	0.73	86:14	0.037	19	1.4

[a]Reactions were carried out at 27 °C in CD_2Cl_2 with 500 mM 2,2,2-trifluoroacetophenone, 50 mM *N*-methylindole or 3-deuterio-*N*-methylindole, and 10 mol % of the indicated catalyst. [b]The product selectivities were determined using *N*-methylindole. [c]Initial rates were used.

https://dx.doi.org/10.1021/acs.joc.0c00498
J. Org. Chem. 2020, 85, 6017–6026

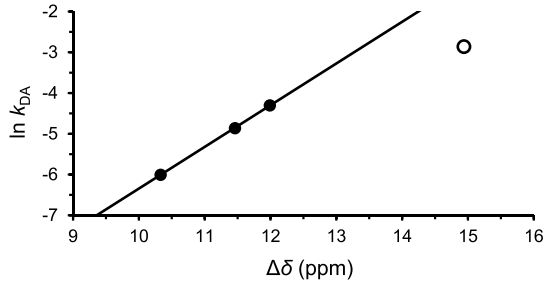

Figure 6. Plot of the logarithm of the rate constant for the Diels–Alder reaction of cyclopentadiene with MVK vs Δδ of the Et_3PO ^{31}P NMR shift for meta-substituted catalysts (filled circles) and the para-isomer **6** (open circle). Linear least-squares fits of the data give ln k = 1.02 × Δδ − 16.6, r^2 = 1.00 (meta isomers only) and ln k = 0.650 × Δδ − 12.4, r^2 = 0.955 (all compounds).

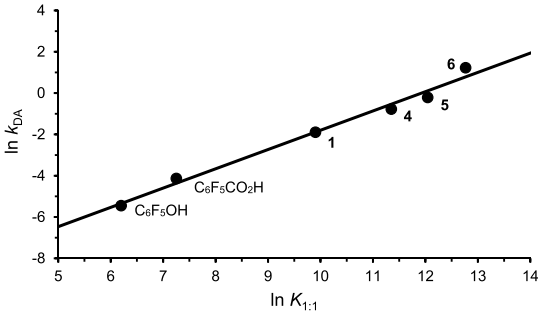

Figure 7. Plot of the logarithm of the rate constant for the Diels–Alder reaction of cyclopentadiene with MVK vs the logarithm of the 1:1 equilibrium binding constants with a colorimetric sensor **7** for all six catalysts in Table 8. The equation for the line obtained from a linear least-squares fit is ln k_{DA} = 0.934 × ln $K_{1:1}$ − 11.1, r^2 = 0.987.

pentafluorobenzoic acid ($C_6F_5CO_2H$) were chosen for this purpose because they have known equilibrium association constants with **7**[10] and Δδ ^{31}P NMR shifts with Et_3PO,[12] and the latter values for pentafluorophenol and pentafluorobenzoic acid are between those for **1** and **4** and **5** and **6**, respectively (Table 8). The UV–vis method, however, suggests that the two noncharged compounds are significantly weaker acids than the hydroxypyridinium salts and should be much less effective catalysts. Kinetic data for both the Friedel–Crafts alkylation of *N*-methylindole with *trans*-β-nitrostyrene and the Diels–Alder reaction of cyclopentadiene with MVK were obtained using both C_6F_5OH and $C_6F_5CO_2H$. The resulting rate constants for the latter reaction are in accord with the $K_{1:1}$ values from the UV–vis titrations in that the two noncharged catalysts are much less effective than **1**, **4**, **5**, and **6**.[17] Both the quantities (k and $K_{1:1}$) span approximately 3 orders of magnitude, and their log–log plot is linear for all six catalysts that were examined (i.e., charged and noncharged, Figure 7). An analogous correlation with the ^{31}P NMR Δδ shifts is not observed, indicating that binding to Et_3PO is not as universal a predictor of reactivity and depends more on the structure of the species being investigated (i.e., compounds with the same Δδ values can have different acidities and catalytic activities). This is in agreement with the report by Diemoz and Franz, who found separate correlations for different types of compounds.[12]

If one uses the Friedel–Crafts rate constants for the transformation of *N*-methylindole with *trans*-β-nitrostyrene rather than those for the Diels–Alder reaction of cyclopentadiene with MVK in the log–log plot displayed in Figure 7, then a parabolic relationship results rather than a straight line (Figure 8). The maximum rate is obtained with **5** and falls off with more or less acidic catalysts as given by bigger or smaller $K_{1:1}$ values, respectively. This indicates that **5**

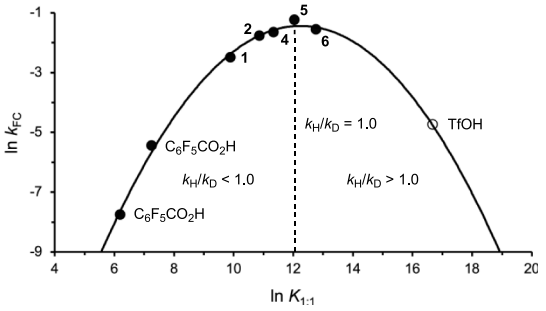

Figure 8. Plot of the logarithm of the rate constant for the Friedel–Crafts reaction of *N*-methylindole with *trans*-β-nitrostyrene vs the logarithm of the 1:1 equilibrium binding constants with a colorimetric sensor **7** (filled circles). A least-squares analysis of the data gives ln k_{DA} = −0.169 × (ln $K_{1:1}$)^2 + 4.15 × ln $K_{1:1}$ − 26.8, r^2 = 0.996, and this quadratic equation was used to obtain an estimated value for ln $K_{1:1}$ for triflic acid (open circle) of 16.6.

represents an inflection point in the mechanism and the rate-determining step shifts from C–C bond formation with weaker acids to proton abstraction with stronger ones (i.e., step 1 vs 3 in Scheme 2). In accord with this view, the KIEs are 1.0 for **5**, <1.0 for weaker acids, and >1.0 for stronger ones. It also appears that the charged hydroxypyridinium ion salts are all more acidic than trifluoroacetic acid (CF_3CO_2H) given that $K_{1:1}$ = 5,490 and ln $K_{1:1}$ = 8.61 for this compound.[10,18]

CONCLUSIONS

Incorporation of electron-withdrawing substituents into charge-containing catalysts proved to be an effective strategy for increasing their acidities in a nonpolar solvent (CH_2Cl_2), as measured by 1:1 equilibrium association constants with **7**, ^{31}P

Table 8. Spectroscopic and Kinetic Data for the Friedel–Crafts and Diels–Alder Reactions with All Catalysts

catalyst	$K_{1:1}$	Δδ (ppm)	k_{FC} (h^{-1})[a]	$t_{1/2}$ (h)	k_{DA} (h^{-1})[b]	$t_{1/2}$ (h)
1	2.0 × 10^4	10.33	0.082	8.5	0.15	4.7
4	8.5 × 10^4	11.46	0.19	3.6	0.46	1.5
5	1.7 × 10^5	11.99	0.29	2.4	0.81	0.85
6	3.5 × 10^5	14.94	0.21	3.3	3.4	0.20
C_6F_5OH	492[c]	11.0[d]	0.00043	1600	0.0043	160
$C_6F_5CO_2H$	1410[c]	12.8[d]	0.0042	160	0.016	43

[a]Reactions were carried out at 27 °C in CD_2Cl_2 with 10 mol % of the indicated catalyst, 500 mM *trans*-β-nitrostyrene, and 50 mM *N*-methylindole. [b]Reactions were carried out at 25 °C in CD_2Cl_2 with 1 mol % of the indicated catalyst, 250 mM cyclopentadiene, and 25 mM MVK. Background-corrected rate constants for the noncatalyzed processes are given. [c]This value was taken from ref 10. [d]This value was taken from ref 12.

https://dx.doi.org/10.1021/acs.joc.0c00498
J. Org. Chem. 2020, 85, 6017–6026

NMR shifts with triethylphosphine oxide, and gas-phase acidities. Of these quantities, the $K_{1:1}$ values were found to be more broadly suitable for correlating catalyst activities. KIEs and an inverted parabolic rate profile for the Friedel–Crafts alkylation of *N*-methylindole with *trans*-*β*-nitrostyrene revealed that the rate-determining step can change from carbon–carbon bond formation to proton transfer to the conjugate base of the catalyst. This leads to a region where the reaction rates decrease with increasing acidity, making this a less useful model transformation for evaluating relative catalyst acidities than previously considered. All of the hydroxypyridinium $BAr^F_4{}^-$ salts reported in this work were also found to be more acidic than trifluoroacetic acid in dichloromethane.

EXPERIMENTAL SECTION

General. All reaction vessels and NMR tubes were stored at 120 °C for a minimum of 12 h and allowed to cool to room temperature in a vacuum desiccator over Drierite before use. Syringes and volumetric flasks were kept in the same desiccator but were not heated. Alumina, molecular sieves, and calcium sulfate were activated in a kiln at 300 °C for at least 24 h.

Acetone, chloroform, and carbon tetrachloride were supplied by Fisher Scientific, whereas ethyl propiolate, 2,2,2-trifluoroacetophenone, and pentafluorobenzoic acid were obtained from Oakwood Chemical. 1-Chloro-2,4-dinitrobenzene, triethylphosphine oxide, sodium tetrakis[3,5-bis(trifluoro-methyl)phenyl]borate ($NaBAr^F_4$), pentafluorophenol, and HCl were purchased from Acros Organics, Alfa Aesar, ArkPharm, Fluka, and VWR Chemical, respectively. Deuterated solvents were acquired from Cambridge Isotope Laboratories, and all other chemicals were purchased from Sigma-Aldrich. Reagents were used as supplied except for *N*-methylindole, which was passed neat through a pipet containing activated alumina and stored under argon. Anhydrous CH_2Cl_2 was used as purchased, CD_2Cl_2 was dried by the addition of activated molecular sieves to the reagent bottle at least 24 h before use, and all other solvents were dried in the same manner as *N*-methylindole and stored over molecular sieves. Charged catalysts were kept under vacuum (0.05–0.1 Torr) for at least 12 h before use.

NMR spectra were recorded using 400 and 500 MHz spectrometers. The ^1H and ^{13}C chemical shifts were referenced at δ 5.32 and 54.0 (CD_2Cl_2), δ 7.26 and 77.2 ($CDCl_3$), δ 2.50 and 39.5 (DMSO-d_6), and δ 1.94 and 1.3 (CD_3CN), respectively. ^2H chemical shifts were referenced relative to benzene-d_6 (7.36 ppm). Triethylphosphine oxide ^{31}P NMR shifts were acquired in CD_2Cl_2 and referenced at δ 50.5 through the deuterium lock channel according to the IUPAC unified scale.[19] Medium-pressure liquid chromatography (MPLC) was performed using an automated flash chromatography system with silica gel columns. Melting point data were collected in unsealed capillaries and were uncorrected. Solution and attenuated total reflection (ATR)–Fourier transform IR spectroscopy spectra were recorded with a liquid cell and a laminated diamond crystal, respectively. High-resolution mass spectra were recorded on an electrospray ionization-time of flight mass spectrometer using PEG-200 as an internal mass calibrant. UV spectra were recorded using 10 mm quartz cells sealed with polytetrafluoroethylene (PTFE) septum caps.

***N*-Methyl-3-hydroxypyridinium (1).** The iodide and $BAr^F_4{}^-$ salts of this ion were prepared according to the literature procedure.[5d]

***(E)*-*N*-(2-Carboethoxyvinyl)-3-hydroxypyridinium BAr^F_4 (2).** Concentrated HCl (1.75 mL, 21.0 mmol) was added dropwise with stirring to a 50 mL round-bottomed flask containing 3-hydroxypyridine (0.99 g, 10.5 mmol) and 25 mL of methanol. After 10 min, the solvent was removed in vacuo, and the resulting solid was dissolved in ethanol (30 mL). Ethyl propiolate (1.60 mL, 1.55 g, 15.8 mmol) was added, and this mixture was heated with an oil bath to reflux overnight. Concentration of the resulting material with a rotary evaporator afforded a residue that was dissolved in 25 mL of acetone. This solution was stirred overnight at room temperature, and the resulting precipitate was isolated by vacuum filtration to give 845 mg (35%) of crude **2-Cl**. Some of this material (64.7 mg, 0.282 mmol), along with 1.5 mL of CH_2Cl_2 and 250 mg (0.28 mmol) of $NaBAr^F_4$, were added to a 6 dram vial and stirred overnight at room temperature. The resulting precipitate was removed with a 0.45 μm PTFE membrane, and then hexanes were added until the solution just became cloudy. This mixture was subsequently dried over activated $CaSO_4$ and filtered through another 0.45 μm PTFE membrane. Removal of the solvent in vacuo gave 253 mg (85%) of an off-white powder (mp 175–178 °C) that was stored in a dry box under nitrogen. ^1H NMR (400 MHz, CD_2Cl_2): δ 8.35 (dd, J = 2.2, 1.7 Hz, 1H), 8.28 (ddd, J = 6.0, 1.2, 1.2 Hz, 1H), 8.10 (ddd, J = 8.8, 2.5, 1.0 Hz, 1H), 8.05 (d, J = 13.9 Hz, 1H), 7.99 (dd, J = 8.8, 6.0 Hz, 1H), 7.72 (s, 8H), 7.56 (s, 4H), 6.74 (d, J = 14.0 Hz, 1H), 4.37 (q, J = 7.1 Hz, 2H), 1.36 (t, J = 7.1 Hz, 3H). $^{13}C\{^1H\}$ NMR (125 MHz, CD_2Cl_2): δ 162.5, 162.3 (q, $^1J_{B-C}$ = 62 Hz), 158.4, 141.5, 136.0, 135.4, 133.8, 130.2, 130.1, 129.4 (qq, $^2J_{F-C}$ = 39 Hz and $^2J_{B-C}$ = 3.5 Hz), 125.2 (q, $^1J_{F-C}$ = 339 Hz), 123.8, 118.1 (septet, $^3J_{F-C}$ = 4.6 Hz), 63.6, 14.3. IR–ATR: 3103, 1704, 1358, 1280, 1121 cm^{-1}. HRMS (ESI) m/z: $[M - BAr^F_4]^+$ calcd for $C_{10}H_{12}NO_3$, 194.0812; found, 194.0829.

***n*-Octyl (*E*)-3-Chloroacrylate.** Propiolic acid (3.0 mL, 3.41 g, 48 mmol) was added over 1 min to a 25 mL round-bottomed flask containing 5 mL (60 mmol) of concentrated HCl. This solution was then heated with an oil bath to reflux with stirring for 18 h before being diluted with 5 mL of water. The product was extracted with chloroform (3 × 5 mL), and the combined organic material was washed with brine (2 × 5 mL) and dried over $MgSO_4$. Concentration in vacuo gave 4.72 g (90%) of crude (*E*)-3-chloroacrylic acid as an odorous, lustrous brown solid (flakes). A portion of this material (450 mg, 4.1 mmol), along with 700 μL (580 mg, 4.5 mmol) of *n*-octanol and 160 mg (0.84 mmol) of *p*-toluenesulfonic acid monohydrate, was placed in a 25 mL round-bottomed flask equipped with a Dean–Stark trap and dissolved in 7.5 mL of toluene. This solution was heated with an oil bath to 130 °C for 24 h, during which time water was removed from the system. Concentration of the reaction mixture with a rotary evaporator was followed by the addition of 15 mL of hexanes and filtration of the resulting material. Removal of the solvent in vacuo afforded an oil that was purified by MPLC with 5% ethyl acetate in hexanes to give 829 mg (92%) of a clear, pale yellow liquid. The ^1H NMR spectrum of this previously reported compound matched the literature data.[20] ^1H NMR (400 MHz, $CDCl_3$): δ 7.35 (d, J = 13.5 Hz, 1H), 6.24 (d, J = 13.5 Hz, 1H), 4.15 (t, J = 6.7 Hz, 2H), 1.65 (p, J = 7.6 Hz, 2H), 1.39–1.22 (m, 10H), 0.88 (t, J = 6.7 Hz, 3H).

***(E)*-*N*-(2-Carbooctoxyvinyl)-3-hydroxypyridinium Chloride (3-Cl).** In a 25 mL round-bottomed flask, 779 mg (3.56 mmol) of *n*-octyl (*E*)-3-chloroacrylate and 271 mg (2.85 mmol) of 3-hydroxypyridine were dissolved in 5 mL of acetonitrile. This solution was heated to reflux with an oil bath with stirring for 24 h, and then an additional 162 mg (0.741 mmol) of *n*-octyl (*E*)-3-chloroacrylate was added. The reaction was heated for another 12 h and was subsequently concentrated with a rotary evaporator. Ethyl acetate (10 mL) was added to the resulting dark brown oil, and the mixture was stirred at room temperature for 4 h. This resulted in precipitation of the product, which was collected by vacuum filtration to afford 385 mg (43%) of a pale tan powder (mp 132–134 °C) that was stored in a dry box under nitrogen. ^1H NMR (400 MHz, $CDCl_3$): δ 9.31 (s, 1H), 8.59 (s, 1H), 8.33–8.20 (m, 2H), 7.95 (s, 1H), 6.95 (d, J = 13.4 Hz, 1H), 4.23 (t, J = 6.7 Hz, 2H), 1.70 (p, J = 6.8 Hz, 2H), 1.41–1.20 (m, 10H), 0.87 (t, J = 6.8 Hz, 3H). $^{13}C\{^1H\}$ NMR (156 MHz, $CDCl_3$): δ 163.3, 159.4, 142.3, 136.1, 132.8, 130.2, 128.9, 121.5, 66.7, 31.9, 29.30, 29.28, 28.6, 25.9, 22.8, 14.2. IR–ATR: 2958, 2928, 2855, 2473 (OH···Cl$^-$), 1710, 1582, 1317, 1289, 1185 cm^{-1}. HRMS (ESI) m/z: $[M - Cl]^+$ calcd for $C_{16}H_{24}NO_3$, 278.1751; found, 278.1768.

***(E)*-*N*-(2-Carbooctoxyvinyl)-3-hydroxypyridinium BAr^F_4 (3).** Dichloromethane (1 mL) was added to a 6 dram vial containing 565 mg (0.638 mmol) of $NaBAr^F_4$ and 200 mg (0.637 mmol) of **3-Cl**, and the solution was stirred at room temperature overnight. Filtration of the resulting mixture through a 0.45 μm PTFE membrane and removal of the solvent under reduced pressure gave 720 mg (99%) of

https://dx.doi.org/10.1021/acs.joc.0c00498
J. Org. Chem. 2020, 85, 6017–6026

the product as an orange-brown semisolid. This material degraded with a half-life of approximately 5 days when stored in a dry box under nitrogen. ^{1}H NMR (400 MHz, CD_2Cl_2): δ 8.34 (t, J = 2.0 Hz, 1H), 8.21 (dt, J = 6.0 and 2.0 Hz, 1H), 8.08 (ddd, J = 8.8, 2.5, and 1.0 Hz, 1H), 8.03 (d, J = 14.0 Hz, 1H), 7.89 (dd, J = 8.8 and 6.0 Hz, 1H), 7.75−7.70 (m, 8H), 7.57 (s, 4H), 6.73 (d, J = 14.0 Hz, 1H), 4.30 (t, J = 6.8 Hz, 2H), 1.73 (p, J = 7.4 Hz, 2H), 1.45−1.25 (m, 10H), 0.88 (t, J = 7.0 Hz, 3H). ^{13}C{^{1}H} NMR (125 MHz, $CDCl_3$) 162.1, 161.8 (q, $^1J_{B-C}$ = 62 Hz), 158.1, 140.9, 135.1, 134.9, 132.5, 129.4, 129.2 (qq, $^2J_{F-C}$ = 39 Hz and $^2J_{B-C}$ = 3.8 Hz), 129.3, 124.6 (q, $^1J_{F-C}$ = 338 Hz), 123.3, 117.7, 67.6, 31.8, 29.21, 29.17, 28.4, 25.8, 22.7, 14.1. IR−ATR: 3084, 2933, 2861, 1706, 1582, 1355, 1277, 1127 cm^{-1}. HRMS (ESI) m/z: [M − BAr^F_4]$^+$ calcd for $C_{16}H_{24}NO_3$, 278.1751; found, 278.1759.

***N*-(2,4-Dinitrophenyl)-3-hydroxypyridinium BAr^F_4 (4).** In a 50 mL round-bottomed flask, 320 mg (3.4 mmol) of 3-hydroxypyridine and 690 mg (3.4 mmol) of 1-chloro-2,4-dinitrobenzene were dissolved in 20 mL of acetonitrile and heated to reflux with an oil bath with stirring overnight. After cooling to room temperature, the resulting precipitate was collected by vacuum filtration and washed with acetonitrile to give 959 mg (96%) of crude **4-Cl** as a light tan powder. A portion of this material (112 mg, 0.377 mmol) was dissolved in 5 mL of water with 300 mg (0.34 mmol) of $NaBAr^F_4$ in a 6 dram vial. Dichloromethane (5 mL) was added, and the mixture was stirred vigorously for 3 h. The clear yellow organic layer was subsequently washed with brine (2 × 5 mL) and dried over $MgSO_4$. It was then triturated with hexanes until the solution just became cloudy whereupon it was passed through a 0.45 μm PTFE membrane. Removal of the solvent in vacuo gave 328 mg (86%) of a light tan powder (mp 54−56 °C) that was stored in a dry box under nitrogen. ^{1}H NMR (400 MHz, CD_2Cl_2): δ 9.30 (d, J = 2.4 Hz, 1H), 8.85 (dd, J = 8.6 and 2.4 Hz, 1H), 8.25−8.19 (m, 2H), 8.14 (ddd, J = 6.0, 1.4, and 1.3 Hz, 1H), 8.07 (dd, J = 8.6 and 5.9 Hz, 1H), 7.93 (d, J = 8.6 Hz, 1H), 7.72 (s, 8H), 7.55 (s, 4H). ^{13}C{^{1}H} NMR (125 MHz, CD_2Cl_2): δ 162.3 (q, $^1J_{B-C}$ = 62 Hz), 159.7, 150.7, 143.7, 138.6, 136.7, 135.6, 135.4, 133.4, 131.1, 130.7, 130.0, 129.4 (qq, $^2J_{F-C}$ = 39 Hz and $^2J_{B-C}$ = 3.7 Hz), 125.2 (q, $^1J_{F-C}$ = 339 Hz), 123.6, 118.1 (septet, $^3J_{F-C}$ = 5.0 Hz). IR−ATR: 3114, 1694, 1611, 1553, 1481, 1354, 1279 cm^{-1}. HRMS (ESI) m/z: [M − BAr^F_4]$^+$ calcd for $C_{11}H_8N_3O_5$, 262.0458; found, 262.0467.

***(E)*-*N*-(2-Cyanovinyl)-3-hydroxypyridinium BAr^F_4 (5).** A solution of 5.0 mL (4.1 g, 76 mmol) of acrylonitrile in 5 mL of chloroform was prepared in a 25 mL round-bottomed flask fitted with a condenser topped with an addition funnel. This setup was covered in aluminum foil to avoid exposure to light and heated to reflux with an oil bath. Bromine (9.0 mL, 28 g, 153 mmol) was then added dropwise over 1 h, and the reaction mixture was refluxed for an additional 3 h. It was subsequently washed with 10% aqueous $Na_2S_2O_3$ (3 × 5 mL) and brine (2 × 5 mL) and then dried with Na_2SO_4. Rotary evaporation of the organic material afforded 16.1 g (98%) of crude 2,3-dibromopropionitrile as a golden oil. A portion of this material (470 mg, 2.2 mmol) was dissolved in 7 mL of methanol along with 420 mg (4.4 mmol) of 3-hydroxypyridine in a 25 mL round-bottomed flask. This mixture was heated to reflux with an oil bath for 3 h and concentrated with a rotary evaporator to give a dark brown viscous oil, which was combined with 7 mL of isopropanol and stirred vigorously at room temperature overnight. The precipitate that formed was isolated by vacuum filtration, dissolved in 2 mL of methanol, and triturated into toluene (20 mL) with stirring. Vacuum filtration of the resulting solid gave 288 mg (57%) of crude **5-Br** as a brown powder. Some of this material (67.2 mg, 0.290 mmol) was placed in a 6 dram vial along with 1 mL of water with 210 mg (0.24 mmol) of $NaBAr^F_4$. Dichloromethane (1 mL) was added, and the mixture was stirred overnight at room temperature. The organic layer was subsequently washed with brine (2 × 2 mL) and dried over Na_2SO_4. At a later date, it was triturated with hexanes until the solution just became cloudy, dried over activated $CaSO_4$, and passed through a 0.45 μm PTFE membrane. Removal of the solvent under reduced pressure afforded 221 mg (91%) of a brown, slightly lustrous powder (mp 157−160 °C) that was stored in a dry box under nitrogen. ^{1}H NMR (400 MHz, CD_2Cl_2): δ 8.29 (dd, J = 2.0 and 1.4 Hz, 1H), 8.23 (d, J = 6.0 Hz, 1H), 8.17 (ddd, J = 9.1, 2.7, and 0.9 Hz, 1H), 8.04 (dd, J = 8.8 and 6.0 Hz, 1H), 7.87 (d, J = 14.4 Hz, 1H), 7.72 (s, 8H), 7.56 (s, 4H), 6.38 (d, J = 14.3 Hz, 1H). ^{13}C{^{1}H} NMR (125 MHz, CD_2Cl_2): δ 162.3 (q, $^1J_{B-C}$ = 62 Hz), 158.8, 145.5, 137.1, 135.4, 133.4, 130.6, 129.7, 129.4 (qq, $^2J_{F-C}$ = 39 Hz and $^2J_{B-C}$ = 3.6 Hz) 125.2 (q, $^1J_{F-C}$ = 339 Hz), 118.1 (septet, $^3J_{F-C}$ = 5.0 Hz), 112.1, 104.8. IR−ATR: 3208, 1355, 1278, 1123 cm^{-1}. HRMS (ESI) m/z: [M − BAr^F_4]$^+$ calcd for $C_8H_7N_2O$, 147.0553; found, 147.0540.

***N*-(2,4-Dinitrophenyl)-4-hydroxypyridinium BAr^F_4 (6).** A 50 mL round-bottomed flask was loaded with 200 mg (2.1 mmol) of 4-hydroxypyridine, 492 mg (2.4 mmol) of 1-chloro-2,4-dinitrobenzene, and 10 mL of acetonitrile. This solution was heated to reflux with an oil bath with stirring overnight, and the resulting precipitate was collected by vacuum filtration and washed with acetonitrile to give 588 mg (94%) of **6-Cl** as a pale pink powder. In a 6 dram vial, 100 mg (0.336 mmol) of this material was dissolved in 3 mL of methanol along with 298 mg (0.336 mmol) of $NaBAr^F_4$, and the mixture was stirred vigorously. After 30 min, 3 mL of CH_2Cl_2 was added to the vial and stirred overnight continuously. The resulting precipitate was removed with a 0.45 μm PTFE syringe filter, and hexanes were added dropwise to the solution until it just became cloudy. Drying with activated $CaSO_4$, followed by a second filtration and concentration with a rotary evaporator, afforded 340 mg (90%) of an off-white powder (mp 125−127 °C). ^{1}H NMR (400 MHz, CD_2Cl_2): δ 9.27 (d, J = 2.5 Hz, 1H), 8.82 (dd, J = 8.6 and 2.5 Hz, 1H), 8.27−8.23 (m, 2H), 7.88 (d, J = 8.6 Hz, 1H), 7.72 (s, 8H), 7.56 (s, 4H), 7.50−7.46 (m, 2H). ^{13}C{^{1}H} NMR (125 MHz, CD_2Cl_2): δ 174.4, 162.3 (q, $^1J_{B-C}$ = 62 Hz), 160.0, 150.5, 145.6, 138.3, 135.4, 131.3, 131.1, 129.4 (qq, $^2J_{F-C}$ = 39 Hz and $^2J_{B-C}$ = 3.6 Hz), 125.2 (q, $^1J_{F-C}$ = 338 Hz), 123.5, 118.1 (septet, $^3J_{F-C}$ = 4.7 Hz), 116.8. IR−ATR: 3676, 3086, 1643, 1610, 1552, 1355, 1278, 1119 cm^{-1}. HRMS (ESI) m/z: [M − BAr^F_4]$^+$ calcd for $C_{11}H_8N_3O_5$, 262.0458; found, 262.0468.

3-Deuterio-*N*-methylindole.[15] Using CH_2Cl_2 as an eluent, 1 mL (8.0 mmol) of *N*-methylindole was passed through a small column of activated alumina. This solution was then concentrated with a rotary evaporator, and the resulting material was stored in a 6 dram vial under argon. Concurrently, a 50 mL two-necked round-bottomed flask equipped with a reflex condenser was filled with D_2O (10 mL) and heated to 110 °C with an oil bath for 1 h, while the system was flushed with argon. The solvent was then removed via a syringe, and *N*-methylindole was added along with 15 mL of D_2O. This mixture was heated to 80 °C with vigorous stirring under argon for 24 h and then stirred for an additional 96 h at room temperature. The product was subsequently extracted with CH_2Cl_2 (1 × 15 mL), and the organic layer was dried over $MgSO_4$. The solution was concentrated in vacuo, and the resulting neat liquid was passed through a plug of activated alumina to give 657 mg (62%) of a pale mint green oil (99% D by ^{1}H NMR) that was stored in a glovebox under nitrogen. ^{1}H NMR (400 MHz, CD_2Cl_2): δ 7.60 (d, J = 7.9 Hz, 1H), 7.35 (d, J = 8.2 Hz, 1H), 7.21 (t, J = 7.2 Hz, 1H), 7.11−7.06 (m, 2H), 6.47 (d, J = 3.1 Hz, 0.01 H), 3.79 (s, 3H).

General Friedel−Crafts Kinetic Procedures. To a 1 mL volumetric flask, 74.6 mg (0.500 mmol) of *trans*-β-nitrostyrene or 70.2 μL (87.0 mg, 0.500 mmol) of 2,2,2-trifluoroacetophenone was added along with 6.2 μL (6.5 mg, 0.050 mmol) of *N*-methylindole and 0.005 mmol of a charged catalyst or 10 μL of a 0.5 M solution of a noncharged catalyst in CH_2Cl_2. This mixture was diluted with CD_2Cl_2 to the mark and mixed by inverting the flask twice. It was then transferred to an NMR tube which was capped and sealed with a PTFE tape. The first NMR spectrum was collected within 5 min of the preparation of the solvent (t_0), and the NMR tube was maintained at 27 °C in the NMR probe (for KIE experiments) or a water bath (for all other experiments) between acquisition of subsequent spectra. When *trans*-β-nitrostyrene was used as the electrophile, the reaction progress was monitored using signals at δ 6.47 (*N*-methylindole) and δ 5.17, 5.08, and 4.98 (Friedel−Crafts product) or δ 3.79 (3-*d*-*N*-methylindole) and δ 3.74 (deuterated product) for the KIE experiments. With $PhCOCF_3$ as the electrophile, the methyl signals at 3.79 (*N*-methylindole), 3.83 (mono addition product), and 3.74 ppm (bis addition product) were used. A pseudo-first-order kinetic

https://dx.doi.org/10.1021/acs.joc.0c00498
J. Org. Chem. 2020, 85, 6017−6026

model was employed to determine half-lives and rate constants (Tables S1–S4 and Figures S1 and S2).

General Procedure for the Reaction of Cyclopentadiene with MVK. Cyclopentadiene was generated by distillation from its dimer and stored at −78 °C under argon for up to 3 h. MVK was distilled within 1 week of its use and was kept at 4 °C under argon. A 1 mL volumetric flask was filled with MVK (20.3 μL, 17.5 mg, 0.250 mmol), 0.0025 mmol of a charged catalyst, or 10 μL of a 0.25 M solution of a noncharged catalyst in CH_2Cl_2, and sufficient CH_2Cl_2 before being mixed by inverting the stoppered flask twice. A portion of this solution (100 μL) was added to a separate 1 mL volumetric flask along with 21.0 μL (16.5 mg, 0.250 mmol) of cyclopentadiene and filled with CD_2Cl_2 before mixing this mixture by inverting the flask twice. This solution was then transferred to an NMR tube that was capped and sealed with a PTFE tape. The first NMR spectrum was collected within 5 min of solvent addition (t_0), and the NMR tube was maintained at 25 °C in the NMR probe between acquisition of subsequent spectra. The reaction progress was monitored using signals at 2.24 (MVK), 2.08 (endo), and 2.17 ppm (exo) (Table S5 and Figure S3). A pseudo-first-order kinetic model was used to determine half-lives and rate constants.

Solution IR Procedure. A 6 dram vial was loaded with **3** (29.2 mg, 25.6 μmol), CCl_4 (5 mL), and CD_3CN (50 μL), and this mixture was stirred until all of the catalyst dissolved. A separate solution of 5 mL of CCl_4 and 50 μL of CD_3CN with no catalyst was also prepared, and a background spectrum of this mixture was recorded in a 10 mm liquid cell that was stored in a dry box under nitrogen. This cell was subsequently emptied and purged with nitrogen for 1 min before being reloaded with the sample solution. A new spectrum was obtained and background-corrected.

General Procedure for UV–Vis Titrations. 7-Methyl-2-phenylimidazo[1,2-*a*]pyrazin-3(7*H*)-one (**7**) was kept under vacuum (0.05–0.1 Torr) for at least 12 h before use. Three volumetric flasks were employed to prepare the required solutions as follows: a 1 mL volumetric flask was filled with 1.0–1.5 mg (4.4–6.7 μmol) of **7** and sufficient CH_2Cl_2 to afford solution A. In a 5 mL volumetric flask, 25 μL of solution A was diluted with CH_2Cl_2 to the line to give solution B. A separate 5 mL volumetric flask was used to prepare solution C, which consisted of 25 μL of solution A, 25–30 molar equivalents of the catalyst relative to **7**, and sufficient CH_2Cl_2 to fill the flask to the line. Background UV–vis spectra of CH_2Cl_2 from 300 to 950 nm were collected before each sample spectrum in a 10 mm quartz cuvette with a screw-on PTFE septum cap. For the titrations, 2 mL of solution B was placed in a separate cuvette, and the UV–vis spectrum was recorded. Subsequently, 10 μL of solution C was added via a syringe, and the solution was swirled for 15 s and a new spectrum was obtained. Further mixing of the solution for an additional 10 s was carried out, and the spectrum was re-recorded. This was repeated, if necessary, until consecutive spectra differed by no more than 1 nm in λ_{max} and 0.010 absorbance units. Additional aliquots of solution C were added, and the spectra were recorded in the same way until λ_{max} did not change over three consecutive additions (**1**, **2**, **4**, and **5**) or until at least 20 molar equivalents of catalyst relative to **7** had been added (**6**). Equilibrium binding constants (K) were determined using absorbance values at 440, 470, 500, and 530 nm by carrying out nonlinear fits of the resulting binding isotherms using the Supramolecular BindFit app (app.supramolecular.org/bindfit).[21] In each case, 1:1, 2:1, and 1:2 associations were explored, though all of the data are in accord with 1:1 binding except for the results with **6**, which are consistent with 1:2 binding (Table S6). While λ_{max} for the 1:1 complex can be obtained directly in the former instances, it cannot be obtained in the latter case. Consequently, $\lambda_{max(1:1)}$ was determined by plotting $\chi_{1:1}/\lambda_{max}$ versus $\chi_{1:1}$, where $\chi_{1:1}$ is the mole fraction of the 1:1 complex obtained from the BindFit output file.[22] The reciprocal of the sum of the slope and y-intercept from the resulting linear least-squares fit afforded $\lambda_{max(1:1)}$. These values are all within 1.0 nm of the directly observed, leveled-off determinations with **1**, **2**, **4**, and **5**.

Catalyst Titration Procedures with Triethylphosphine Oxide. Triethylphosphine oxide was stored and weighed in a glovebox under nitrogen. For the titration with **1**, 2.1–2.4 mg (15.7–17.9 μmol) of Et_3PO was dissolved in minimal CH_2Cl_2, transferred to a 1 mL volumetric flask, and diluted to the mark (solution A). In a separate 1 mL volumetric flask, **1** (9.4–10.0 mg, 9.7–10.3 μmol) was added and diluted to the line with CH_2Cl_2 (solution B). An NMR tube was then filled with 100 μL of solution A and 400 μL of CD_2Cl_2. An initial NMR spectrum was obtained to establish the ^{31}P chemical shift of Et_3PO. Subsequently, 80 μL of solution B was added via a microsyringe to the NMR tube, which was then inverted twice before obtaining another spectrum. This process was repeated until the ^{31}P signal shifted by no more than 0.1 ppm in three consecutive spectra (Table S7 and Figure S15). For the other catalysts, full titrations were not carried out. In these cases, 5.0 mg (37.3 μmol) of Et_3PO was placed in a 1 mL volumetric flask that was filled to the line with CH_2Cl_2. An NMR tube was loaded with 135 μL of this solution and 315 μL of CD_2Cl_2 to obtain the initial ^{31}P NMR signal of Et_3PO. Subsequently, 7.5 μmol of the selected catalyst and 500 μL of CH_2Cl_2 were added with mixing, and a second ^{31}P NMR spectrum was recorded to obtain the change in the chemical shift.

Computations. Calculations were performed at the Minnesota Supercomputing Institute using Gaussian 16[23] with the B3LYP functional and the 6-31G+(d,p) basis set.[24] Full geometry optimizations and subsequent vibrational frequency determinations were carried out, and all of the given stationary points correspond to energy minima with no negative eigenvalues (Table S8). Unscaled vibrational frequencies were used to obtain zero-point energies, thermal corrections to the enthalpies at 298 K, and entropies. Low-frequency modes that contribute more than $1/2RT$ to the enthalpy correction were replaced with $1/2RT$.

■ ASSOCIATED CONTENT

Supporting Information

The Supporting Information is available free of charge at https://pubs.acs.org/doi/10.1021/acs.joc.0c00498.

Kinetic, UV–vis titration, and Ph_3PO ^{31}P chemical shift data; plots of ln $k_{Diels-Alder}$ versus ln $K_{1:1}$ and ΔG°_{acid}; NMR spectra; and computed structures and energies, and the complete citation to ref 23 (PDF)

■ AUTHOR INFORMATION

Corresponding Author

Steven R. Kass − *Department of Chemistry, University of Minnesota, Minneapolis, Minnesota 55455, United States;* orcid.org/0000-0001-7007-9322; Email: kass@umn.edu

Author

George F. Riegel − *Department of Chemistry, University of Minnesota, Minneapolis, Minnesota 55455, United States*

Complete contact information is available at: https://pubs.acs.org/10.1021/acs.joc.0c00498

Notes

The authors declare no competing financial interest.

■ ACKNOWLEDGMENTS

Generous support from the National Science Foundation (CHE-1665392) and the Minnesota Supercomputing Institute for Advanced Computational Research is gratefully acknowledged.

■ REFERENCES

(1) (a) Akiyama, T. Stronger Brønsted Acids. *Chem. Rev.* **2007**, *107*, 5744–5758. (b) Akiyama, T.; Mori, K. Stronger Brønsted Acids: Recent Progress. *Chem. Rev.* **2015**, *115*, 9277–9306.

(2) (a) Schreiner, P. R. Metal-Free Organocatalysis Through Explicit Hydrogen Bonding Interactions. *Chem. Soc. Rev.* **2003**, *32*, 289–296.

(b) Doyle, A. G.; Jacobsen, E. N. Small-Molecule H-Bond Donors in Asymmetric Catalysis. *Chem. Rev.* **2007**, *107*, 5713−5743. (c) Giacalone, F.; Gruttadauria, M.; Agrigento, P.; Noto, R. Low-Loading Asymmetric Organocatalysis. *Chem. Soc. Rev.* **2012**, *41*, 2406−2447. (d) Phipps, R. J.; Hamilton, G. L.; Toste, F. D. The Progression of Chiral Anions From Concepts to Applications in Asymmetric Catalysis. *Nat. Chem.* **2012**, *4*, 603−614. (e) Wende, R. C.; Schreiner, P. R. Evolution of Asymmetric Organocatalysis: Multi- and Retrocatalysis. *Green Chem.* **2012**, *14*, 1821−1849. (f) Auvil, T. J.; Schafer, A. G.; Mattson, A. E. Design Strategies for Enhanced Hydrogen-Bond Donor Catalysts. *Eur. J. Org. Chem.* **2014**, 2633−2646.

(3) (a) Akiyama, T.; Itoh, J.; Yokota, K.; Fuchibe, K. Enantioselective Mannich-Type Reaction Catalyzed by a Chiral Brønsted Acid. *Angew. Chem., Int. Ed.* **2004**, *43*, 1566−1568. (b) Akiyama, T.; Morita, H.; Itoh, J.; Fuchibe, K. Chiral Brønsted Acid Catalyzed Enantioselective Hydrophosphonylation of Imines: Asymmetric Synthesis of α-Amino Phosphonates. *Org. Lett.* **2005**, *7*, 2583−2585. (c) Lippert, K. M.; Hof, K.; Gerbig, D.; Ley, D.; Hausmann, H.; Guenther, S.; Schreiner, P. R. Hydrogen-Bonding Thiourea Organocatalysts: The Privileged 3,5-Bis(trifluoromethyl)-phenyl Group. *Eur. J. Org. Chem.* **2012**, 5919−5927. (d) Zhang, Z.; Bao, Z.; Xing, H. N,N′-Bis[3,5-bis(trifluoromethyl)phenyl]thiourea: A Privileged Motif For Catalyst Development. *Org. Biomol. Chem.* **2014**, *12*, 3151−3162. (e) Yao, Y.; Shu, H.; Tang, B.; Chen, S.; Lu, Z.; Xue, W. Synthesis, Characterization and Application of Some Axially Chiral Binaphthyl Phosphoric Acids in Asymmetric Mannich Reaction. *Chim. J. Chem.* **2015**, *33*, 601−609. (f) Zhou, F.; Yamamoto, H. A Powerful Chiral Phosphoric Acid Catalyst for Enantioselective Mukaiyama-Mannich Reactions. *Angew. Chem., Int. Ed.* **2016**, *55*, 8970−8974.

(4) (a) Jensen, K. H.; Sigman, M. S. Systematically Probing the Effect of Catalyst Acidity in a Hydrogen-Bond-Catalyzed Enantioselective Reaction. *Angew. Chem., Int. Ed.* **2007**, *46*, 4748−4750. (b) Jensen, K. H.; Sigman, M. S. Evaluation of Catalyst Acidity and Substrate Electronic Effects in a Hydrogen Bond-Catalyzed Enantioselective Reaction. *J. Org. Chem.* **2010**, *75*, 7194−7201. (c) Li, X.; Deng, H.; Zhang, B.; Li, J.; Zhang, L.; Luo, S.; Cheng, J.-P. Physical Organic Study of Structure−Activity−Enantioselectivity Relationships in Asymmetric Bifunctional Thiourea Catalysis: Hints for the Design of New Organocatalysts. *Chem.—Eur. J.* **2010**, *16*, 450−455. (d) Kaupmees, K.; Tolstoluzhsky, N.; Raja, S.; Rueping, M.; Leito, I. On the Acidity and Reactivity of Highly Effective Chiral Brønsted Acid Catalysts: Establishment of an Acidity Scale. *Angew. Chem., Int. Ed.* **2013**, *52*, 11569−11572.

(5) (a) Samet, M.; Buhle, J.; Zhou, Y.; Kass, S. R. Charge-Enhanced Acidity and Catalyst Activation. *J. Am. Chem. Soc.* **2015**, *137*, 4678−4680. (b) Fan, Y.; Kass, S. R. Electrostatically Enhanced Thioureas. *Org. Lett.* **2016**, *18*, 188−191. (c) Ma, J.; Kass, S. R. Electrostatically Enhanced Phosphoric Acids: A Tool in Brønsted Acid Catalysis. *Org. Lett.* **2016**, *18*, 5812−5815. (d) Payne, C.; Kass, S. R. Structural Considerations for Charge-Enhanced Brønsted Acid Catalysts. *J. Phys. Org. Chem.* **2020**, *33*, No. e4069.

(6) Jung, M. E.; Buszek, K. R. The Stereochemistry of Addition of Trialkylammonium and Pyridinium Tetrafluoroborate Salts to Activated Acetylenes. Preparation of Novel Dienophiles for Diels−Alder Reactions. *J. Am. Chem. Soc.* **1988**, *110*, 3965−3969.

(7) Katritzky, A. R.; Rahimi-Rastgoo, S.; Sabongi, G. J.; Fischer, G. W. 1,3-Dipolar Character of Six-Membered Aromatic Rings. Part 51. Cycloadditions of 1-(β-Benzoylvinyl)-3-Oxidopyri-diniums and Subsequent Transformations. *J. Chem. Soc., Perkin Trans. 1* **1980**, 362−

(8) [illegible]O.; Kupetis, G. K.; Rastenyté, L.; Matijo, A. A Convenient Preparation of 1-Vinylpyridinium Salts. *Synthesis* **1999**, [illegible]

(9) Eda, M.; Kurth, M. J.; Nantz, M. H. The Solid-Phase Zincke Reaction: Preparation of ω-Hydroxy Pyridinium Salts in the Search for CFTR Activation. *J. Org. Chem.* **2000**, *65*, 5131−5135.

(10) (a) Huynh, P. N. H.; Walvoord, R. R.; Kozlowski, M. C. Rapid Quantification of the Activating Effects of Hydrogen-Bonding Catalysts with a Colorimetric Sensor. *J. Am. Chem. Soc.* **2012**, *134*, 15621−15623. (b) Walvoord, R. R.; Huynh, P. N. H.; Kozlowski, M. C. Quantification of Electrophilic Activation by Hydrogen-Bonding Organocatalysts. *J. Am. Chem. Soc.* **2014**, *136*, 16055−16065.

(11) The λ_{max} values are not as good a measure of catalyst acidity or activity.

(12) Diemoz, K. M.; Franz, A. K. NMR Quantification of Hydrogen-Bond-Activating Effects for Organocatalysts Including Boronic Acids. *J. Org. Chem.* **2019**, *84*, 1126−1138.

(13) (a) Herrera, R. P.; Sgarzani, V.; Bernardi, L.; Ricci, A. Catalytic Enantioselective Friedel-Crafts Alkylation of Indoles with Nitroalkenes by Using a Simple Thiourea Organocatalyst. *Angew. Chem., Int. Ed.* **2005**, *44*, 6576−6579. (b) Ganesh, M.; Seidel, D. Catalytic Enantioselective Additions of Indoles to Nitroalkenes. *J. Am. Chem. Soc.* **2008**, *130*, 16464−16465. (c) Itoh, J.; Fuchibe, K.; Akiyama, T. Chiral Phosphoric Acid Catalyzed Enantioselective Friedel−Crafts Alkylation of Indoles with Nitroalkenes: Cooperative Effect of 3 Angstrom Molecular Sieves. *Angew. Chem., Int. Ed.* **2008**, *47*, 4016−4018. (d) Hermeke, J.; Toy, P. H. Phosphonium Ion Tagged Chiral Phosphoric Acids and Their Application in Friedel−Crafts Reactions of Indoles. *Tetrahedron* **2011**, *67*, 4103−4109. (e) Marqués-López, E.; Alcaine, A.; Tejero, T.; Herrera, R. P. Enhanced Efficiency of Thiourea Catalysts by External Brønsted Acids in the Friedel−Crafts Alkylation of Indoles. *Eur. J. Org. Chem.* **2011**, 3700−3705. (f) Shokri, A.; Wang, X.-B.; Kass, S. R. Electron-Withdrawing Trifluoromethyl Groups in Combination with Hydrogen Bonds in Polyols: Brønsted Acids, Hydrogen-Bond Catalysts, and Anion Receptors. *J. Am. Chem. Soc.* **2013**, *135*, 9525−9530.

(14) (a) Cooper, J. D.; Vitullo, V. P.; Whalen, D. L. Evidence for a Change in Rate-Determining Step of the Acid-Catalyzed Hydrolysis of a Vinyl Ether. *J. Am. Chem. Soc.* **1971**, *93*, 6294−6296. (b) Sayer, J. M.; Jencks, W. P. Mechanism and Catalysis of 2-Methyl-3-thiosemicarbazone Formation. A Second Change in Rate-Determining Step and Evidence for a Stepwise Mechanism for Proton Transfer in a Simple Carbonyl Addition Reaction. *J. Am. Chem. Soc.* **1973**, *95*, 5637−5649. (c) Okuyama, T.; Komoguchi, S.; Fueno, T. Reaction of Thiols with Phenylglyoxal to Give Thiolesters of Mandelic Acid. 2. Intramolecular General-Base Catalysis and Change in Rate-Determining Step. *J. Am. Chem. Soc.* **1982**, *104*, 2582−2587. (d) Jiang, Y.-Y.; Liu, T.-T.; Zhang, R.-X.; Xu, Z.-Y.; Sun, X.; Bi, S. Mechanism and Rate-Determining Factors of Amide Bond Formation through Acyl Transfer of Mixed Carboxylic−Carbamic Anhydrides: A Computational Study. *J. Org. Chem.* **2018**, *83*, 2676−2685.

(15) This compound previously was reported and a similar procedure was employed. For further details, see: Wang, S.; Nie, J.; Zheng, Y.; Ma, J.-A. A Direct Copper-Promoted Three-Component Entry to Trifluoromethylketoximes. *Org. Lett.* **2014**, *16*, 1606−1609.

(16) (a) Wang, Y.; Yuan, Y.; Xing, C.-H.; Lu, L. Trifluoromethanesulfonic Acid-Catalyzed Solvent-Free Bisindolylation of Trifluoromethyl Ketones. *Tetrahedron Lett.* **2014**, *55*, 1045−1048. (b) Liu, X.-D.; Wang, Y.; Ma, H.-Y.; Xing, C.-H.; Yuan, Y.; Lu, L. Cs_2CO_3-Catalyzed Alkylation of Indoles with Trifluoromethyl Ketones. *Tetrahedron* **2017**, *73*, 2283−2289. (c) Ma, J.; Kass, S. R. Asymmetric Arylation of 2,2,2-Trifluoroacetophenones Catalyzed by Chiral Electrostatically-Enhanced Phosphoric Acids. *Org. Lett.* **2018**, *20*, 2689−2692.

(17) This also applies to the Friedel−Crafts reaction rate constants.

(18) Unfortunately, we were unable to measure the corresponding quantity for triflic acid as the solution became opaque when 1 equiv of TfOH was added to a 1.0×10^{-6} M solution of **7** in CH_2Cl_2.

(19) Harris, R. K.; Becker, E. D.; Cabral de Menezes, S. M.; Goodfellow, R.; Granger, P. NMR Nomenclature. Nuclear Spin Properties and Conventions for Chemical Shifts (IUPAC Recommendations 2001). *Pure Appl. Chem.* **2001**, *73*, 1795−1818.

(20) Miura, K.; Sugimoto, J.; Oshima, K.; Utimoto, K. Triethylborane Induced Radical Reaction of Ketene Silyl Acetals with Polyhalomethanes. *Bull. Chem. Soc. Jpn.* **1992**, *65*, 1513−1521.

https://dx.doi.org/10.1021/acs.joc.0c00498
J. Org. Chem. 2020, 85, 6017−6026

(21) (a) Thordarson, P. Determining Association Constants From Titration Experiments in Supramolecular Chemistry. *Chem. Soc. Rev.* **2011**, *40*, 1305−1323. (b) Hibbert, D. B.; Thordarson, P. The Death of the Job Plot, Transparency, Open Science and Online Tools, Uncertainty Estimation Methods and Other Developments in Supramolecular Chemistry Data Analysis. *Chem. Commun.* **2016**, *52*, 12792−12805. (c) Also, see: http://supramolecular.org
(22) For additional details, see ref 5d.
(23) Frisch, M. J.; Trucks, G. W.; Schlegel, H. B.; Scuseria, G. E.; Robb, M. A.; et al. *Gaussian 16*; Gaussian, Inc.: Wallingford CT, 2016.
(24) (a) Becke, A. D. Density-Functional Thermochemistry. III. The Role of Exact Exchange. *J. Chem. Phys.* **1993**, *98*, 5648−5652. (b) Lee, C.; Yang, W.; Parr, R. G. Development of the Colle-Salvetti Correlation-Energy Formula into a Functional of the Electron Density. *Phys. Rev. B: Condens. Matter Mater. Phys.* **1988**, *37*, 785−789.

https://dx.doi.org/10.1021/acs.joc.0c00498
J. Org. Chem. 2020, 85, 6017−6026